Spectrochimica Acta Part A: Molecular and Biomolecular Spectroscopy 257 (2021) 119804

Contents lists available at ScienceDirect

Spectrochimica Acta Part A: Molecular and Biomolecular Spectroscopy

journal homepage: www.elsevier.com/locate/saa

Simultaneous measurement of liquid film thickness and temperature on metal surface

Weiwei Wu [a], Shuaishuai Kong [a], Xiaoyan Xu [a], Jin Tao [b], Chuanliang Li [c], Jingyi Wang [a], Mingxu Su [a], Huinan Yang [a,*]

[a] School of Energy and Power Engineering, University of Shanghai for Science and Technology, Shanghai 200093, China
[b] State Key Laboratory of Applied Optics, Changchun Institute of Optics, Chinese Academy of Sciences, Changchun 130033, China
[c] Taiyuan University of Science and Technology, Taiyuan 030000, China

HIGHLIGHTS

- Simultaneous measurement of liquid film thickness and temperature on metal surface.
- The DLAS film thickness and temperature with maximum deviations of 3.3% and 2.0%.
- Evaporation of films with initial thicknesses (490.0/624.6/744.5 μm) were studied.
- Flow of films at initial temperatures (40.0/60.0/80.0 °C) were researched.

GRAPHICAL ABSTRACT

The determined thicknesses (a_1) (solid square: DLAS; hollow square: UPEM) and temperatures (a_2) (solid triangle: DLAS; hollow triangle: thermocouple) of dynamic liquid films formed with water in the tank at 40.0 °C on the inclined metal plate.

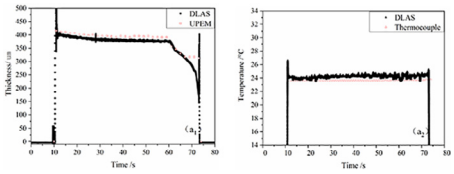

ARTICLE INFO

Article history:
Received 25 January 2021
Received in revised form 17 March 2021
Accepted 6 April 2021
Available online 9 April 2021

Keywords:
Measurement
Liquid film
Diode laser absorption spectroscopy
Thickness
Temperature

ABSTRACT

The flow and evaporation of liquid films widely exist in various industrial fields. The investigation into liquid films is essential to design and optimize the relevant industrial processes. In this work, a simultaneous measurement method of liquid film thickness and temperature on metal surface based on diode laser absorption spectroscopy (DLAS) was proposed, and a corresponding measurement system was developed. First, static liquid films of 200–800 μm on the horizontal metal plate were studied, ultrasonic pulse-echo method (UPEM) and thermocouple were employed to compare with DLAS data. It revealed that the relative deviations of film thicknesses and temperatures measured by different methods were 3.3% and 2.0%, respectively. Furthermore, the evaporation processes of static liquid films were investigated. For the liquid films with different initial thicknesses (490.0/624.6/744.5 μm), the average relative deviations of the film thicknesses and temperatures measured by different methods were 0.1%/0.8%/4.1% and 0.1%/2.6%/3.0%, respectively. Finally, the flow processes of liquid films at different initial temperatures (40.0/60.0/80.0 °C) on the inclined metal plate were researched. It was found that the variation trends of the liquid film thicknesses and temperatures measured by different methods were in good agreement. In the stable stages of flow processes, the average relative deviations of liquid film thicknesses and temperatures measured by different methods were 9.0%/8.4%/5.1% and 3.6%/1.2%/2.5%, respectively. This work is helpful to understand the heat and mass transfer mechanisms in the evaporation and flow processes of liquid films.

1. Introduction

The flow and evaporation of liquid films widely exist in energy, chemical engineering, and other industrial fields. For example, flow

* Corresponding author.
E-mail address: yanghuinan@usst.edu.cn (H. Yang).

https://doi.org/10.1016/j.saa.2021.119804
1386-1425/

of falling film on the horizontal corrugated pipe [1], flow of the film in the passive containment cooling system [2], evaporation of falling film on the vertical evaporator heating tube [3] and the horizontal pipe in the seawater desalination [4], etc. Since the variations of film thicknesses and temperatures inevitably influenced on the heat and mass transfer effects in the relevant industrial equipment, the measurement of these two parameters is helpful to fundamentally understand the relevant mechanisms. Guo et al. [5] found that the liquid films played a primary role in flow boiling process in the micro-channel, and the film thickness affected the thermal load of the fluid greatly. Chauris et al. [6] presented that film thickness was inversely proportional to the heat transfer coefficient in the evaporation process of thin film on capillary heated tube. And Li et al. [7] proposed that the falling film temperature significantly contributed to the film evaporation mass transfer in the duct.

In order to optimize the relevant industrial processes and provide reliable data for simulations, simultaneous measurement of liquid film thickness and temperature with high precision is essential. Traditional measurement methods of liquid film thickness were mainly classified into electrical methods [8–9], acoustic methods [10–11] and optical methods [12–14]. For example, Jaworek et al. [9] utilized a capacitance sensor to determine the liquid film thickness on the pipe wall. However, the measured liquid should be with high conductivity. Jiao et al. [11] obtained the lubricating oil film thickness between mechanical elements with ultrasonic measurement method, but it was difficult to distinguish the echoes from two interfaces of the liquid film less than 150 μm. Chang et al. [12] measured the liquid film thickness on the aircraft by planar laser induced fluorescence method, but the measurement system was complex, and specific tracer should be selected. Thermal resistance and thermocouple are conventional methods for liquid temperature measurement, but the status of liquid film is affected by these invasive methods. Therefore, non-invasive measurement methods were developed by many researchers. Jiang et al. [15] measured the liquid film temperature with thermal infrared imaging technology, and Mignot et al. [16] determined the liquid film thickness and temperature in the condensation and re-evaporating environment by mid-wave infrared absorption method. However, the measurement accuracy was limited by the resolution of the camera and the quality of the captured image. Pan et al. [17] obtained the thickness, temperature, and concentration of static liquid film on quartz glass plate by near infrared absorption spectroscopy, but it was not appropriate for dynamic liquid film on the metal surface.

Therefore, a novel method was proposed to simultaneously measure liquid film thickness and temperature on metal surface based on diode laser absorption spectroscopy (DLAS). The static liquid films (200–800 μm) on the metal plate were firstly investigated by the developed DLAS system, ultrasonic pulse-echo method (UPEM) and thermocouple were employed to validate the developed system. Furthermore, a series of experiments were performed to analyze the processes of static liquid films evaporation with different initial thicknesses on horizontal metal surface and the processes of dynamic liquid films flow at different initial temperatures on inclined metal surface.

2. Theoretical strategy

Based on the Beer-Lambert law, when the light at a specific wavenumber v is reflected by a liquid film on a metal surface, considering the influence of the reflection at the liquid film surface, the transmittance can be expressed as [18],

$$\tau(v) = I_t'/(I_0 - I_s) = \exp[(-n)\sigma(v)\cdot L)] \quad (1.1)$$

where I_0 is the incident light intensity, I_s is the reflected light intensity at the liquid film surface, I_t' represents the light intensity reflected at the metal surface and then refracted on the liquid film surface, n is the molar concentration, and $\sigma(\nu)$ denotes the infrared absorption cross section, and L is the optical path length.

The molar concentration can be obtained as follows:

$$n = \rho(T)/M \quad (1.2)$$

Liquid water was investigated in this work, M is the molar mass, the density ρ is depended on liquid temperature T and can be obtained by following formula [19],

$$\rho(T) = 0.73694 + 0.00199T - 3.73881 \times 10^{-6}T^2 \quad (1.3)$$

In our previous work, the absorption spectra of liquid water at different temperatures (25–75 °C) in the near-infrared range (5800–7800 cm^{-1}) were measured by a Fourier-transform infrared (FTIR) spectrometer [20], and it was found that $\sigma(v)$ was closely relevant to T. Two diode lasers available in the laboratory (center wavelengths λ: 1420 and 1488 nm) were employed. In the future work, other wavenumber positions can be chosen and combined to eliminate non-specific attenuations and improve the measurement accuracy. In order to avoid the interference of water vapor absorption on the measurement of liquid film, the absorption spectra of water vapor near the center wavelengths of the two diode lasers (6718.0–6723.0 cm^{-1} and 7040.0–7044.0 cm^{-1}) were simulated by the HITRAN database. The temperature was 25.0 °C, the optical path length was 10 cm, the pressure was 1 atm, and the water vapor concentration was 0.01 mol/L. As shown in Fig. 1, in the case that water absorption was negligible, two wavenumbers at 6721.6 cm^{-1} and 7040.8 cm^{-1} were selected.

For the two wavenumber positions at 6721.6 cm^{-1} and 7040.8 cm^{-1}, there is a linear relationship between $\sigma(\nu)$ and T:

$$\sigma(v_i) = a_i + b_i T, i = 1, 2 \quad (1.4)$$

where a_i and b_i are the corresponding fit coefficients (as shown in Table. 1). The coefficients of determination R^2 at 6721.6 cm^{-1} and 7040.8 cm^{-1} are 0.999 and 0.994, respectively. It revealed that there was a good linear relationship between $\sigma(\nu)$ and T, as shown in Fig. 2.

Assume that:

$$r = \ln[\tau(v_1)]/\ln[\tau(v_2)] \quad (1.5)$$

The film temperature T can be described as:

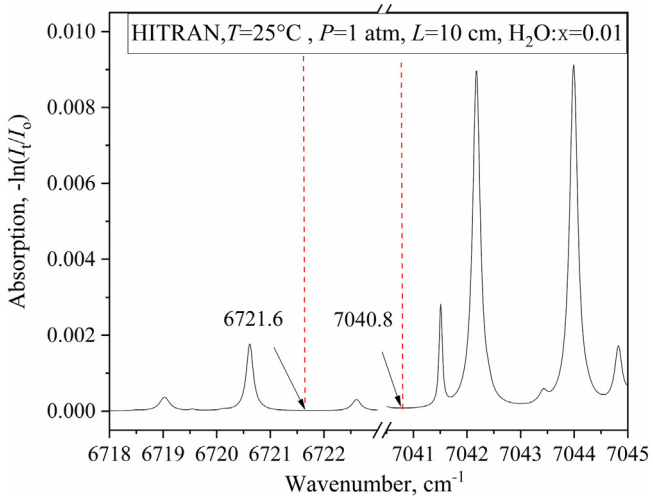

Fig. 1. Simulated absorption spectra of water vapor (6718.0–6723.0 cm^{-1} and 7040.0–7044.0 cm^{-1}).

Table 1
The fit coefficients of $\sigma(\nu)$ and T.

i	ν/ cm^{-1}	a_i	b_i	R^2
1	6721.6	452.96	−1.22	0.994
2	7040.8	380.37	2.85	0.999

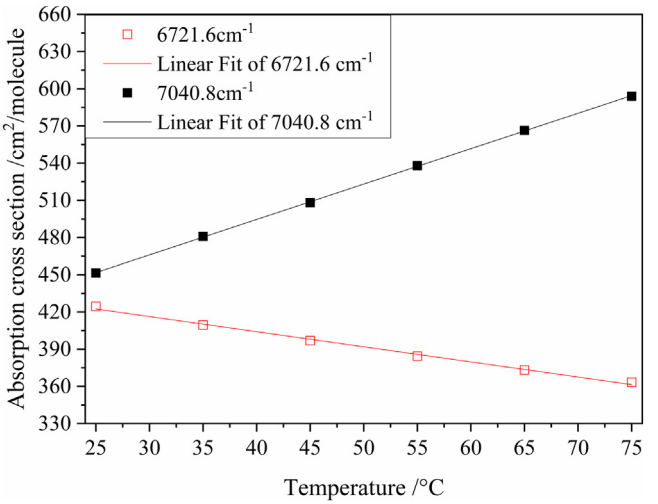

Fig. 2. Fit curves of $\sigma(\nu)$ and T at 6721.6 cm^{-1} and 7040.8 cm^{-1}.

$$T = (a_1 - a_2 r)/(b_2 r - b_1) \tag{1.6}$$

When T was obtained, L can be determined by following formula:

$$L = M \cdot \ln(\tau(\nu))/[(-(a + bT)) \cdot \rho(T)] \tag{1.7}$$

Owing to the geometric relationship between the film thickness d and L, d can be calculated by:

$$d = 1/2\cos\left\{\sin^{-1}[\sin\theta \cdot (n_0/n_1)]\right\} \cdot L \tag{1.8}$$

where θ is the incident angle of the light, n_0 and n_1 are the refractive indexes of air and liquid water, respectively.

This method is also applicable to other liquids, but the absorption spectra of the investigated liquid at different temperatures should be known in advance.

3. Experimental setups and results

3.1. Validation

In order to determine the measurement accuracy of the proposed method, a DLAS system was employed. As depicted in Fig. 3, the temperature and current of the diode lasers (Thorlabs, LM14S2) were tuned by the laser controller (Thorlabs, PRO8000). The two light beams with the center wavenumber positions at 6721.6 cm^{-1} and 7040.8 cm^{-1} were coupled by a wavelength division multiplexer (Thorlabs, TDQ1315HF). It was found in our previous research that the incident angle should be chosen as small as possible [18]. However, the incident angle was fixed at 10° here due to the limitation of the layout of system. The multiplexed light from the collimator (Thorlabs, F280APC-C) was led through the liquid film on a horizontal metal plate, then reflected light was focused by a convex lens (Thorlabs, LB1092-C). A grating (Thorlabs, GR13-0608) was employed to separate the coupled light. The two demultiplexed light beams were received by InGaAs photoelectric detectors (Thorlabs, PDA10CS-EC), and collected by the NI acquisition card (NI, BNC-2110, frequency: 1 kHz). Finally, the data post-processing and real-time display of measurement results were achieved by the LabVIEW (National Instruments) program.

UPEM was employed to determine the liquid film thickness simultaneously and compared with DLAS results. For UPEM, the probe (OLYMPUS, V313-SU, diameter:12.0 mm) was connected to an ultrasonic pulse transmitter and receiver (Panametrics, 5910R). Continuous pulse signal was transmitted, and the reflected signal was received by the probe. The probe was perpendicular to the metal plate and the measurement point 1 of DLAS was in the center of the probe. It should be noted that diameter of DLAS laser beam was only 1 mm, the corresponding measured area was only 0.7% of UPEM probe, and the film thickness measured by UPEM was the average value of the measured area covered by the probe. The temperature obtained by DLAS was compared with the thermocouple data (JINKE, JK840, diameter: 100 μm). The thermocouple was fixed at point 2 keeping 10 mm with point 1 to avoid affecting the optical path and the status of the liquid film.

The deionized water had been deposited 10 times on the surface of the metal plate (150.0 × 150.0 × 30.0 mm, 304 stainless steel) with a needle. A metal ring (diameter:100.0 mm, thickness:10.0 mm) was fixed in the center of the plate to avoid liquid spreading. Then liquid films with different thicknesses were formed. Here, since it was difficult to form liquid films less than 200 μm, and the absorption was saturated at the employed

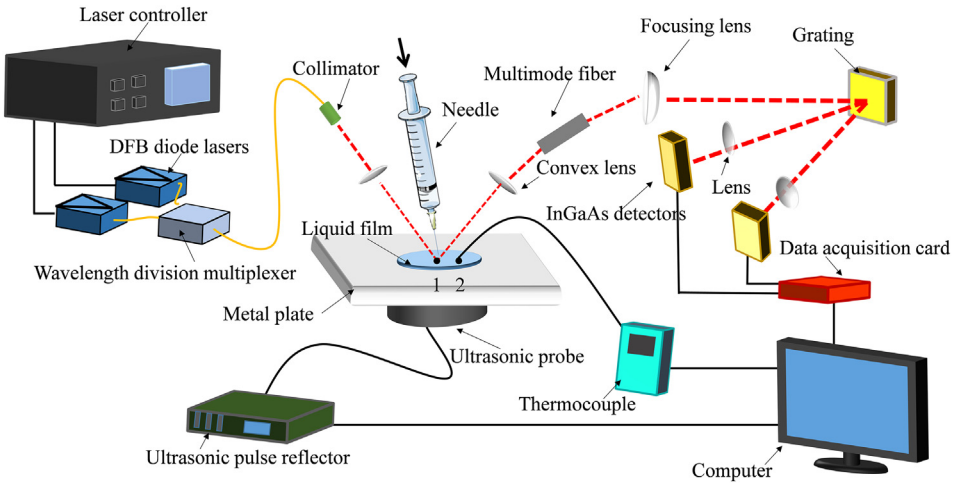

Fig. 3. Schematic drawing of DLAS measurement system.

wavenumber positions when the liquid films were thicker than 800 μm, the validation experiments were only performed with liquid films varied from 200 to 800 μm. It should be pointed out that the thickness variations of liquid films during the evaporation and flow processes in Sections 3.2 and 3.3 were all within this range. For each film thickness, the experiments were repeated for three times. In addition, the experiments were operated at room temperature.

The 10 sets of measured liquid film thicknesses (solid square: DLAS; hollow square: UPEM) and temperatures (hollow triangle: DLAS; solid triangle: thermocouple) on the horizontal metal plate were shown in Fig. 4. It revealed that the maximum standard deviations of film thicknesses and temperatures were 3.58 μm and 0.51 °C for three repeated experiments, respectively. As shown in Fig. 4a, the liquid film thicknesses measured by DLAS and UPEM matched well, it was found that the largest deviation of the film thickness between two methods was 31.7 μm, and the average relative deviation was 3.3%. As shown in Fig. 4b, the average relative deviation of the liquid film temperature measured by DLAS and thermocouple was 2.0%. It revealed that the simultaneous measurement of liquid film thickness and temperature can be achieved by the developed DLAS system with high accuracy.

3.2. The evaporation process of liquid film on the horizontal metal plate

The evaporation process of liquid films with three different initial thicknesses on the horizontal metal plate was investigated. The experimental setup was similar to that shown in Fig. 3. The deionized water was firstly heated by hot air gun (Deli, DL5318), and then injected into the metal plate by the needle. The measured liquid film thicknesses (solid square: DLAS; hollow square: UPEM) and temperatures (solid triangle: DLAS; hollow triangle: thermocouple) were plotted in Fig. 5. As shown in Fig. 5a1, b1, and c1, the three initial film thicknesses measured by DLAS and UPEM were 490.0/624.6/744.5 μm and 488.3/621.7/717.2 μm, respectively. The variation trends of the film thicknesses measured by DLAS were in good agreement with UPEM. The film thicknesses gradually decreased, and the average relative deviations between DLAS and UPEM were 0.1%/0.8%/4.1%, respectively. Due to the surface tension effect, the convex shape of the liquid film was more obvious when the film was thicker, the relative deviation increased. As shown in Fig. 5a2, b2, and c2, the three initial liquid film temperatures measured by DLAS and thermocouple were 33.4/40.2/36.2 °C and 33.9/40.0/36.4 °C, respectively. The variation trends of the liquid film temperatures measured by these two methods matched well, the average relative deviations between the DLAS and thermocouple of three groups were 0.1%/2.6%/3.0%, respectively. It revealed that there were irregular fluctuations of liquid film thicknesses and temperatures during the evaporation processes, it might be caused by the beam steering effects when the small air bubbles appeared and vibrated on the film surface.

3.3. The flow process of liquid film on the inclined metal plate

The measurement system of liquid film on the inclined metal plate was shown in Fig. 6, the arrangement of UPEM and thermocouple was basically same as that in Fig. 3. A water tank (20.0 × 20.0 × 10.0 mm, acrylic) was arranged on the metal plate with an inclination angle of 10° from the optical station, and a flow channel (100.0 × 10.0 mm, acrylic) was fixed on the metal plate. A syringe pump (Shenchen, SPLab02) was connected to the needle and pushed the heated deionized water (40.0/60.0/80.0 °C) into the tank, mass flow rate was adjusted to 4.0 ml/s to ensure that the liquid film was distributed on the plate evenly. Here, the syringe pump was running about 1 min and the experiments were also performed at room temperature.

The measured liquid film thicknesses (solid square: DLAS; hollow square: UPEM) and temperatures (solid triangle: DLAS; hollow triangle: thermocouple) on the inclined metal plate were shown in Fig. 7.The start of the syringe pump (Abbreviation as SOSP) can be defined as the initial time (0 s). As shown in Fig. 7a1, b1, and c1 the liquid film thickness was 0 μm at the start of the data acquisition (0–10 s after SOSP). At this stage, the syringe pump was activated, the water tank was slowly filled and no liquid film was formed on the metal plate. When the front tip of liquid film flowed through the measured point 1, partial light was reflected due to the curvature of the liquid film edge. The attenuation of light intensities was considered as absorption of liquid water, leading to a dramatic increase of liquid film thickness and temperature at ~10 s after SOSP. During the periods (11–60 s after SOSP), the film thickness slowly decreased and reached a relative stable value. The average film thicknesses of the stable stage measured by DLAS and UPEM were 379.2/363.0/384.1 μm and 413.0/393.4/403.5 μm, respectively. The average relative deviations of thicknesses were 9.0%/8.4%/5.1%. Due to the surface tension, the liquid film at the edge of the flow channel was slightly higher than in the center, it led to the overestimation of the film thickness by UPEM. Since the deionized water in the needle had been drained in the periods (60–75 s after SOSP), the remaining deionized water in the tank continued to flow into the flow channel through the slit and the pressure in the tank dropped, the film thickness gradually decreased. In the end, it dropped to be 0 μm (at 75 s after SOSP) due to no supplement of the liquid water.

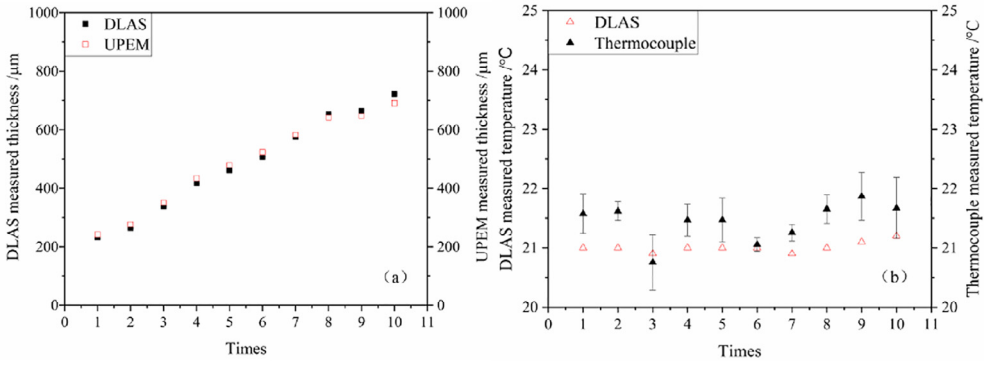

Fig. 4. 10 sets of measured liquid film thicknesses (a) (solid square: DLAS; hollow square: UPEM) and temperatures (b) (solid triangle: DLAS; hollow triangle: thermocouple) on the horizontal metal plate.

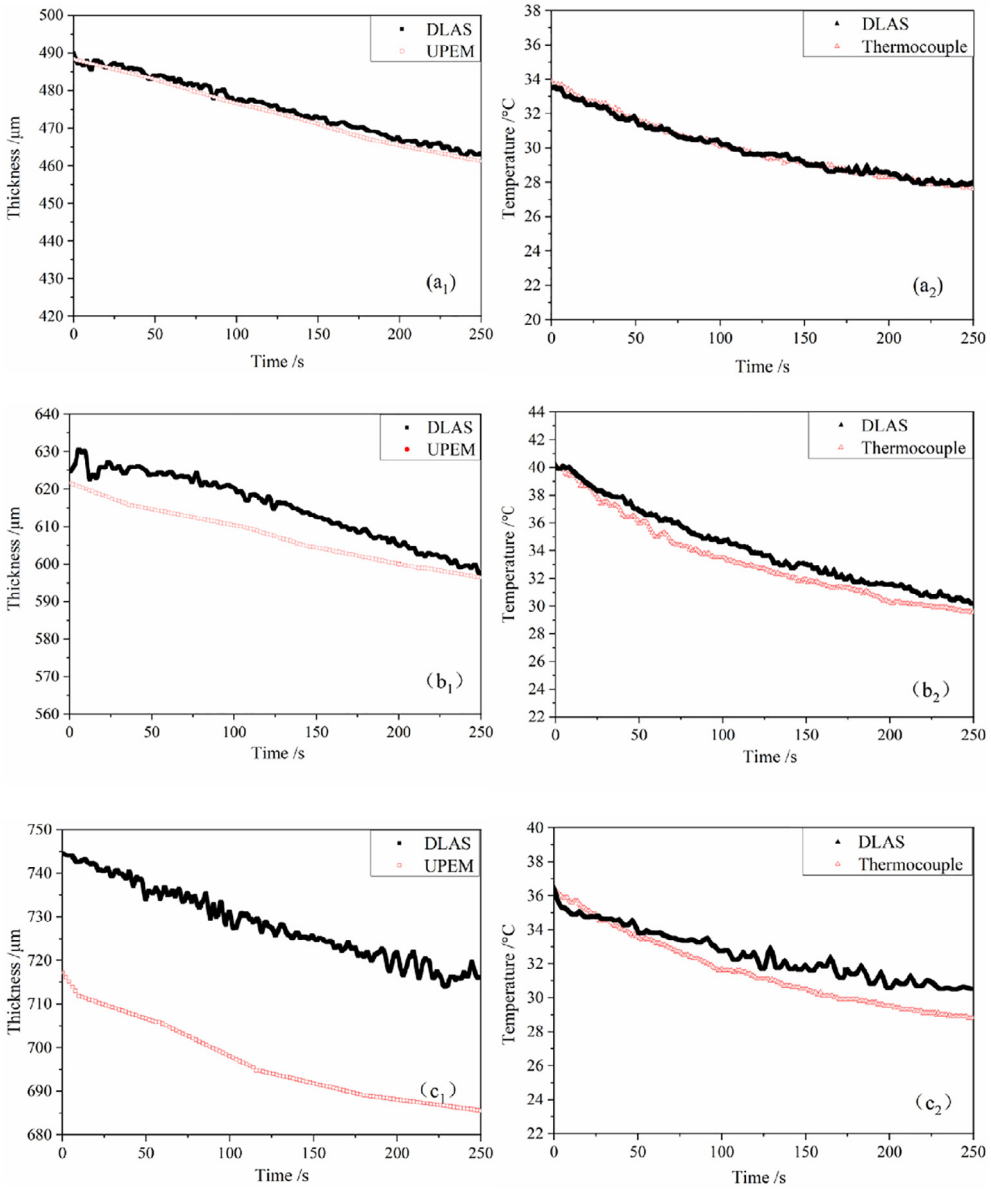

Fig. 5. The determined thicknesses (a_1, b_1, c_1) (solid square: DLAS; hollow square: UPEM) and temperatures (a_2, b_2, c_2) (solid triangle: DLAS; hollow triangle: thermocouple) of liquid films with three different initial thicknesses during evaporation processes on the horizontal metal plate.

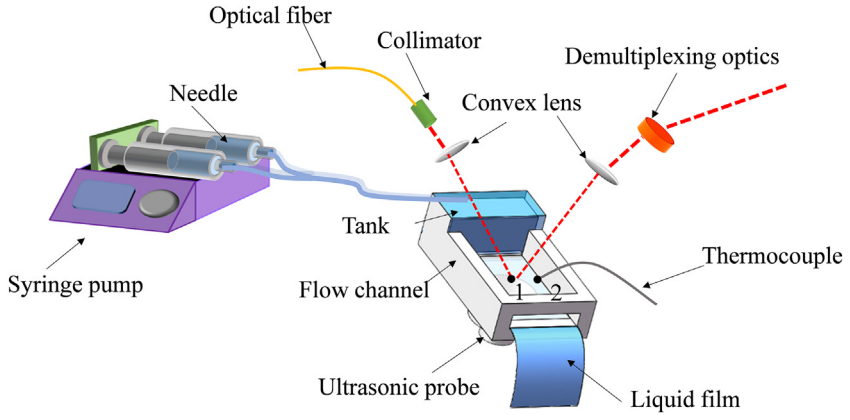

Fig. 6. Measurement system of liquid film on the inclined metal plate.

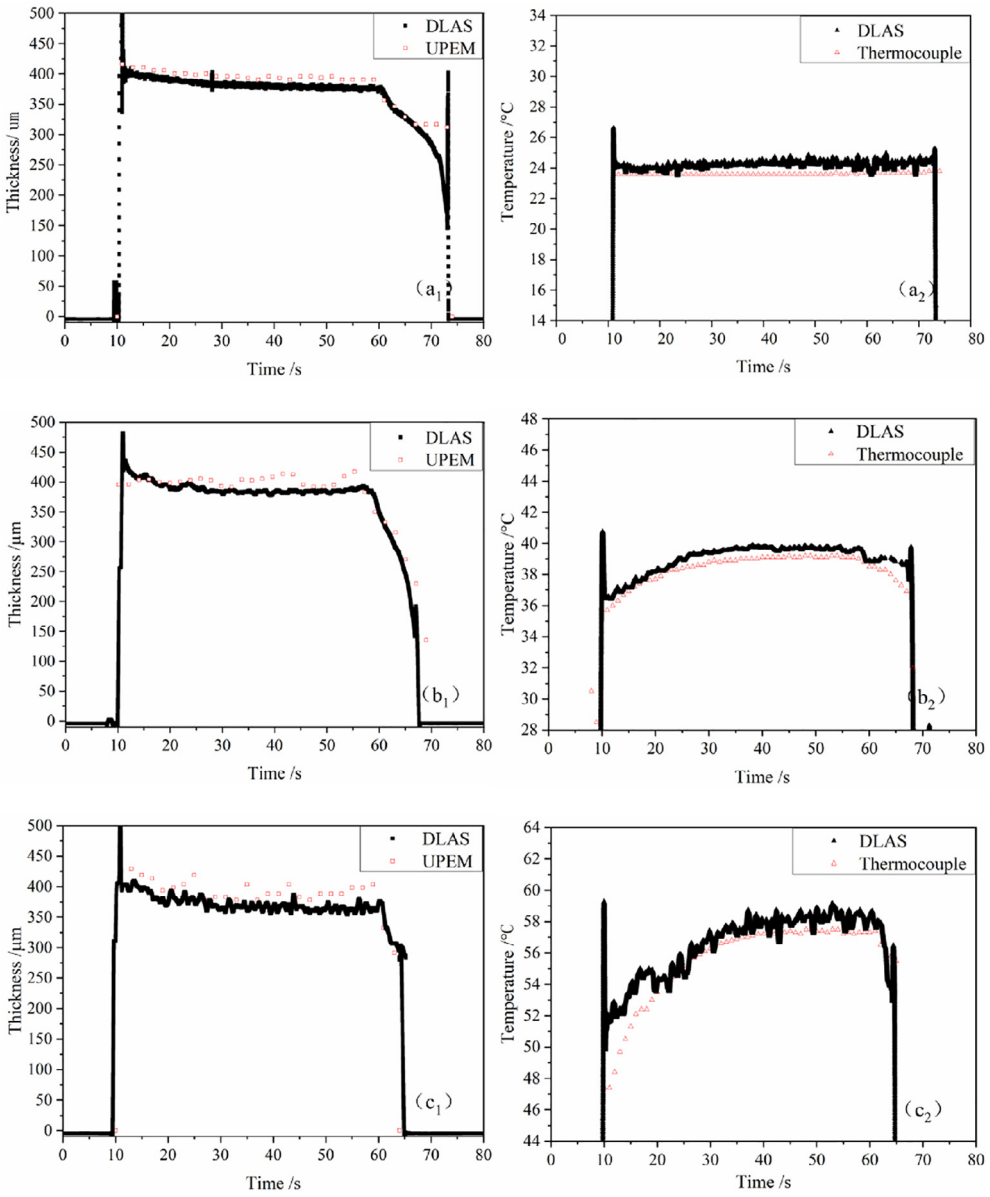

Fig. 7. The determined thicknesses (a_1, b_1, c_1) (solid square: DLAS; hollow square: UPEM) and temperatures (a_2, b_2, c_2) (solid triangle: DLAS; hollow triangle: thermocouple) of dynamic liquid films formed with water in the tank at different temperatures (40.0/60.0/80.0 °C) on the inclined metal plate.

As shown in Fig. 7a2, b2, c2, the liquid film temperatures measured by DLAS and thermocouple at 11.0 s after SOSP were 24.5/36.5/50.0 °C and 23.6/35.7/47.4 °C, respectively. Due to a certain amount of heat loss when the deionized water in the needle flowed through the water tank and the inclined metal plate, the measured data were all lower than the initial heating temperature. As shown in Fig. 7a2, the film temperature was relative stable and the average relative deviation between two methods was 3.6%. Because of the continuous inflow of heated deionized water (11–30 s after SOSP), the liquid film temperature measured by DLAS and thermocouple showed an increasing trend, as shown in Fig. 7b2 and 7c2, and the maximum temperature rise was 3.1 °C and 6.5 °C, respectively. In the process of 30–60 s after SOSP, it revealed that an equilibrium state was reached, and the average relative deviations of film temperatures between two methods were 1.2% and 2.5%, respectively. In the process of 60–75 s after SOSP, the syringe pump stopped and film temperature dropped to be 0 °C.

4. Conclusion

A novel method based on DLAS was proposed to simultaneously measure the liquid film thickness and temperature on the metal surface. The measurement accuracy of the developed DLAS system was validated with static liquid film ranging from 200 to 800 μm on the horizontal metal plate, and the measured results were compared with UPEM and thermocouple. It was found that the average relative deviations of the liquid film thicknesses and temperatures were 3.3% and 2.0%, respectively. The evaporation processes of static liquid films were also investigated. The liquid film thicknesses and temperatures measured by DLAS matched well with UPEM and thermocouple. With the increase of initial liquid film thicknesses, the average relative deviations of film thicknesses and temperature increased. The flow processes of liquid film on the inclined metal plate were also studied, the liquid film thickness slowly decreased and reached a constant value. The variation trends of liquid temperature were in good agreement with thermo-

couple. It indicated that the developed DLAS system can be potentially applied in relevant industrial processes for simultaneous measurement of liquid film thickness and temperature on metal surface. Since quartz tuning fork is used as a novel detector with the advantages of no wavelength limit, low cost and tiny volume [21,22], it can be employed to replace the photodetector to achieve a more reliable and compact system in the future work.

CRediT authorship contribution statement

Weiwei Wu: Conceptualization, Investigation, Software, Validation, Formal analysis, Data curation, Writing - original draft. **Shuaishuai Kong:** Investigation, Software, Writing - review & editing. **Xiaoyan Xu:** Investigation, Software, Writing - review & editing. **Jin Tao:** Resources, Funding acquisition. **Chuanliang Li:** Resources, Funding acquisition. **Jingyi Wang:** Writing - review & editing. **Mingxu Su:** Supervision. **Huinan Yang:** Methodology, Software, Supervision, Writing - review & editing.

Declaration of Competing Interest

The authors declare that they have no known competing financial interests or personal relationships that could have appeared to influence the work reported in this paper.

Acknowledgement

This work was supported by National Natural Science Foundation of China [No. 51676130, U1810129]; the Natural Science Foundation of Shanghai [No. 20ZR1438900], and the Open Foundation of The State Key Laboratory of Applied Optics [No. SKLAO-201909].

References

[1] Y. Zhang, S. Zhang, D. Wang, et al., Flow behavior of liquid falling film on a horizontal corrugated tube, Ann. Nucl. Energy 148 (2020) 107728.
[2] P. Hu, K. Du, S. Zhai, et al., Experiment study of water film/air counter-current flow heat transfer on a vertical plate for passive containment cooling system, Nucl. Eng. Des. 328 (2018) 73–79.
[3] B. Xianbiao, M. Weibin, L. Huashan, Heat and mass transfer of ammonia-water in falling film evaporator, Front. Energy 5 (4) (2011) 358–366.
[4] B. Zhou, B. Liu, D. Yang, et al., Multi-objective optimal operation of coastal hydro-electrical energy system with seawater reverse osmosis desalination based on constrained NSGA-III, Energy Convers. Manage. 207 (2020) 112533.
[5] C. Guo, J. Tao, Y. Jiang, et al., Measurement and theoretical analysis of transient liquid film during micro-channel flow boiling, Int. J. Multiph. Flow 130 (2020) 103365.
[6] N. Chauris, V. Ayel, Y. Bertin, et al., Evaporation of a liquid film deposited on a capillary heated tube: Experimental analysis by infrared thermography of its thermal footprint, Int. J. Heat Mass Transf. 86 (2015) 492–507.
[7] C. Li, Characteristics of the high-temperature water film evaporation with countercurrent turbulent air flow in the duct, Ann. Nucl. Energy 130 (2019) 1–7.
[8] W. Ambrosini, N. Forgione, F. Oriolo, Statistical characteristics of a water film falling down a flat plate at different inclinations and temperatures, Int. J. Multiph. Flow 28 (9) (2002) 1521–1540.
[9] A. Jaworek, A. Krupa, M. Trela, Capacitance sensor for void fraction measurement in water/steam flows, Flow Meas. Instrum. 15 (5–6) (2004) 317–324.
[10] J. Zhang, B.W. Drinkwater, R.S. Dwyer-Joyce, Calibration of the ultrasonic lubricant-film thickness measurement technique, Meas. Sci. Technol. 16 (9) (2005) 1784–1791.
[11] J. Jiao, W. Liu, J. Zhang, et al., Time-frequency analysis for ultrasonic measurement of liquid-layer thickness, Mech. Syst. Sig. Process. 35 (1–2) (2013) 69–83.
[12] S. Chang, W. Yu, M. Song, et al., Investigation on wavy characteristics of shear-driven water film using the planar laser induced fluorescence method, Int. J. Multiph. Flow 118 (2019) 242–253.
[13] A.V. Cherdantsev, J.S. An, A. Charogiannis, et al., Simultaneous application of two laser-induced fluorescence approaches for film thickness measurements in annular gas-liquid flows, Int. J. Multiph. Flow 119 (2019) 237–258.
[14] S.H. Pham, Z. Kawara, T. Yokomine, et al., Measurements of liquid film and droplets of annular two-phase flow on a rod-bundle geometry with spacer, Int. J. Multiph. Flow 70 (2015) 35–57.
[15] B. Jiang, Z. Wang, X. Fu, et al., Experimental Study on Heat Transfer of Heated Falling Film Under Gas-Liquid Cross-Flow Condition, Heat Transf. Eng. 35 (1) (2014) 34–42.
[16] G. Mignot, J. Dupont, S. Paranjape, et al., Measurement of liquid films thickness in a condensing and re-evaporating environment using attenuation of near infrared light, Nucl. Eng. Des. 336 (2018) 64–73.
[17] R. Pan, J.B. Jeffries, T. Dreier, et al., Measurements of liquid film thickness, concentration, and temperature of aqueous urea solution by NIR absorption spectroscopy, Appl. Phys. B-Lasers Opt. 122 (1) (2016) 10.
[18] H. Yang, W. Wei, M. Su, et al., Measurement of liquid water film thickness on opaque surface with diode laser absorption spectroscopy, Flow Meas. Instrum. 60 (2018) 110–114.
[19] D.R. Lide, Handbook of Chemistry and Physics, 75th ed., Taylor & Francis, Florida, 1994.
[20] H. Yang, D. Greszik, T. Dreier, Simultaneous measurement of liquid water film thickness and vapor temperature using near infrared tunable diode laser spectroscopy, App; Phys. B 99 (3) (2010) 385–390.
[21] Y. Ma, Y. Hu, S. Qiao, et al., Trace gas sensing based on multi-quartz-enhanced photothermal spectroscopy, Photoacoustics 20 (2020) 100206.
[22] Y. Hu, S. Qiao, H.Y. He, et al., Quartz-enhanced photoacoustic-photothermal spectroscopy for trace gas sensing, Opt. Express 29 (4) (2021) 5121–5127.